Molecular Dynamics Study of the Inhibition of Monomeric HIV-1 Protease as Alternative to Overcome Drug Resistance by RNA Aptamers

Marzieh Ajamgard,[1,2] Jaber Jahanbin sardroodi, [1,2] and Alireza Rastkar Ebrahimzadeh [1,3,a)]

[1] Molecular Simulation Laboratory (MSL), Azarbaijan Shahid Madani University, Tabriz, Iran.
[2] Department of Chemistry, Faculty of Basic Sciences, Azarbaijan Shahid Madani University, Tabriz, Iran.
[3] Department of Physics, Faculty of Basic Sciences, Azarbaijan Shahid Madani University, Tabriz, Iran.
[a)] Author to whom correspondence should be addressed: a_rastkar@azaruniv.ac.ir

ABSTRACT

Here the interaction of three aptamers with HIV-1 protease has been investigated with the help of molecular dynamics simulations. These simulations lead to precise structural and energetic results. The sequencing of the considered aptamers is AP1 as the aptamer number 1: (CUUCAUUGUAACUUCUCAUAAUUUCCCGAGGCUUUUACUUUCGGGGUCCU), AP2 as the aptamer number 2: (CCGGGUCGUCCCCUACGGGGACUAAAGACUGUGUCCAACCGCCCUCGCCU) and AP3 as the aptamer number 3: (C, U, A, C, and C nucleotides of AP1 were replaced with A, G, G, A, and C to yield AP3). The results of molecular dynamics simulations show that aptamers 2 and 3 are good alternatives to interact with the protease enzyme and to control this enzyme, but in AP2 has somewhat improved the results. The results of MM-PBSA show that although aptamer three as a mutant aptamer has a good affinity with the protease enzyme compared to aptamer one and by impairing dimerization, it disrupts its structural stability and function. However, the results indicate that aptamer 2 is a better inhibitor because it causes a more severe conformational change in the

structure of the enzyme.

I. INTRODUCTION

Due to the high prevalence of human immunodeficiency virus type 1 (HIV-1) disease and drug resistance over the past decades, many investigations have been accomplished on the discovery and introduction of anti-HIV-1 drugs. There are reports of the use of inhibitors as drugs and potent inhibitors[1]. In addition to being potent, these drugs are limited for a long-term purpose, because of their resistance to a variety of viruses[2]. For this reason, there is still a great interest in better understanding of the mechanism of the inhibition to design better drugs. The aim of this research is the theoretical study of HIV-1 protease (PR) inhibition by a new class of antiviral agents. We used RNA aptamers as a protease enzyme inhibitor for potential use in HIV-1 therapy.

Aptamers are short single-stranded structures of RNA or DNA oligonucleotides that have high affinity and selectivity to recognize and bind target molecules[3–8]. These targets are different in size from small molecules to proteins and cells. When they are bound to their targets, aptamers produce complex three-dimensional structures featuring intricate motifs and stable target binding sites[9, 10]. To particular interactions, the ligand can only be bound efficiently with a stable structure[11]. The ligand-specific aptamer can be extracted through an in vitro selection process known as the systematic evolution of ligands by exponential enrichment process (SELEX)[3, 12]. There is relatively little understanding of the mechanisms of ligand binding to aptamers, but it is essential for the full utilization of aptamers as a therapeutic tool[13] and other applications. In the present work, we investigated the orientation and interaction between several aptamers (AP1, AP2 and, AP3) and HIV-1 PR by using molecular dynamics (MD) simulation.

Because HIV-1 PR is an essential enzyme due to its key role in viral maturation, a better understanding of interactions between HIV-1 PR and its specific aptamer remains of great interest to improve drug design. Thus, searching for HIV-1 PR inhibitors as an attractive target in anti-AIDS drug design has become a promising approach. Since inhibition of the enzyme activity by blocking the active site presents only in the dimer, previous studies have suggested that dimer inhibition may overcome the limitation of this inhibition state to prevent inevitable drug resistance[14-17]. By a recent molecular dynamics simulation study, monomeric HIV-1 PR is stable[18], and its folding form is essential for dimer formation. Thus, binding of HIV-1 PR by two folding monomers creates a new site for enzyme inhibition[19]. Hence, in the present work, we used the monomer shape of HIV-1 PR.

This study presents the analysis of interactions between HIV-1 PR and its specific aptamer. The results offer the mechanism of the inhibition of HIV-1 Protease by specific RNA aptamers and the investigation of these structures after simulation. Furthermore, 150 ns MD simulations, for HIV-1 PR and three aptamers and their complex in water, are examined in detail and compared to each other. The results obtained contribute to a better understanding of the mechanism of the inhibition, in particular by combining the methods presented here. Finally, with due attention to the high effectiveness and the proprietary function of non-coding RNA aptamers, we can conclude that these compounds may be suggested as effective HIV-1 anti-protease drugs.

II. METHOD

A. Molecular Dynamics (MD) Simulations

Molecular dynamics (MD) simulation is a powerful technique for the analysis of the interaction between ligand-target[20]. All MD simulations in this paper were performed out with the NAMD2.12 package[21] with CHARMM27 and CHARMM36[22-24] force field for the studied complex with

explicit water. VMD[25] is a molecular visualization program for setting up the molecular dynamics simulation systems. The built molecular systems were simulated under (NVT) and (NPT) ensembles. During hydration, in the initial configuration, a water box containing around 34200, 35589, 54879 water molecules were placed around complex 1, 2 and, 3, respectively. The periodic boundary conditions were applied in all systems with TIP3P[26] model for water. The size of the simulation box (Figure 1) for complex 1 was (65, 81, 77 Å), for complex 2 (91, 80, 84 Å) and complex 3 was (82, 72, 71 Å), as you can see in Figure 1. The MD domain consisted of HIV-1 PR, aptamer, water molecules, and sodium ions. We increase the temperature of the system to 310 K. Then the temperature is kept constant using a Langevin thermostat in 310 K. The pressure was held at a constant value of 1.013125 bar using a Nose-Hoover Langevin piston.

B. Simulation setup and protocol

To remove any bad contacts and to set all bond lengths, bond angles, and torsions of the considered systems, they were minimized at absolute zero before the equilibrium molecular dynamics simulations. After the minimization step, the systems were heated to 310 K and then 150 ns molecular dynamics simulations were executed. The time step for MDS was 1 fs and cut off radii for van der Waals interactions has been set to 16 Å. The temperature and pressure are maintained constant by a Langevin thermostat (310 K) and a Langevin barostat (1.01325 bar), respectively.

C. Preparation of initial structures

The simulations have been performed by using the HIV-1-PR structure reported in Protein Data Bank [PDB] with the id of 1HPP[27]. Recently Duclair et al.[28] showed experimentally that some RNA aptamers and the ones considered here have anti-HIV properties. We named them AP1, AP2, and AP3 for brevity. They have the following nucleotide sequencing AP1:

CUUCAUUGUAACUUCUCAUAAUUUCCCGAGGCUUUUACUUUCGGGGUCCU, AP2: CCGGGUCGUCCCCUACGGGGACUAAAGACUGUGUCCAACCGCCCUCGCCU, AP3: a mutant structure of AP1 in which C-4, U-6, A-18, C-27 and C-38 nucleotides of AP1 were substituted with A, G, G, A, and C. The Second-generation RNA aptamer (see Figure 2A) was selected from Kinefolde web server [29]. The third structures (see Figure 2B) predicted by SIMRNA web server[30] is in agreement with the experimental data. They were the starting point of the performed MD simulation.

D. Structural specifications

The structure of the enzyme molecule consisted of a chain. It included 99 amino acids. HIV-1 PR is a polar structure and contains the hydrophobic residues, generally. The active site of the protease is provided a catalytic Asp-Thr-Gly triad at positions 25 to 27, respectively[28]. Figure 3 shows the structure of the HIV 1 protease monomer.

Aptamers included 1568, 1075, 1005 atoms, a unique nucleic acid chain and 50, 51, 48 residues for AP1, AP2, and AP3, respectively. Each of aptamers 1, 2, and 3 consists of 24, 1, and 22 unbound bases at the 5`-end, 4, 9, and 4 unbound bases at the 3`-end. In AP1 structure, there is a stem region with eight intramolecular base pairs, a symmetric loop. In AP2 structure, there are two stem regions with three intramolecular base pairs and two interior loops and a stem-loop (hairpin loop). In AP3 structure, there is a stem region with four intramolecular base pairs; a symmetric interior loop, and a stem-loop (hairpin loop) and. (see Figure 2A)

D. MM/PBSA Calculations

In order to a deeper understanding of the interactions between HIV-1 RT and considered aptamers, the free energy of binding ($\Delta G_{binding}$), was calculated. The $\Delta G_{binding}$ was investigated using the

following Eq. 1:

$$\Delta G_{binding} = G_{complex} - G_{aptamer} - G_{HIV-1\ PR} \qquad (1)$$

where G is the value of the total free energy. Complex, aptamer, and HIV-1PR have their usual meanings defined in this text.

The total free energy of any species can be calculated from Eq.2:

$$< G > = < E_{MM} > + < G_{solvation} > - TS \qquad (2)$$

In which E_{MM}, $G_{solvation}$, T, and S are molecular mechanics potential energy, the free energy of solvation, temperature (310 K here), and entropy, respectively. The braces show the average values. Following the high computational cost and low prediction accuracy[31-34], the entropy contribution (TS) of the aptamer and enzyme was neglected. The source of this choice is the increased conformational flexibility. Therefore, this increased conformational flexibility could not make a favorable contribution to the interaction between aptamer and enzyme[35].

Furthermore, E_{MM} is defined as the summation of bonding, E_b, and non-bonding, E_{nb}, (electrostatic and van der Waals) interactions:

$$E_{MM} = E_b + E_{nb} \qquad (3)$$

And

$$E_{nb} = E_{elec} + E_{vdw} \qquad (4)$$

Note, in the single trajectory approach, the conformation of protein and ligand in the bound and unbound forms are assumed to be identical. Thus, ΔE_{bonded} is always assumed to be zero[36].

Electrostatic interactions are obtained by coulomb Eq.5:

$$E_{elec}(r_{ij}) = \frac{q_i \cdot q_j}{4 \cdot \pi \cdot \epsilon_0 \cdot r_{ij}} \quad (5)$$

And van der Waals interactions are obtained by Lennard-Jones (LJ) potential function

$$E_{vdw}(r_{ij}) = -4 \cdot \epsilon_{ij}[(\frac{\sigma_{ij}}{r_{ij}})^{12} - (\frac{\sigma_{ij}}{r_{ij}})^{6}] \quad (6)$$

The solvation free energy contribution was calculated with the help of

$$G_{solvation} = G_{pols} + G_{npols} \quad (7)$$

Where pols and npols are polar and non-polar parts of the free energy of solvation, respectively. The non-polar contribution of the solvation free energy expression is derived from SASA-only non-polar model[37] giving G_{npols} as follows:

$$G_{npols} = \gamma(\chi) + \beta \quad (8)$$

Where γ, χ and, β are the surface tension coefficient of the solvent, the SASA of the solute and, β is a constant. The experimental constants γ and β have values of 0.916 Kcal/mol/Å^2 and 0.0054 Kcal/mol, respectively. The polar term was calculated in Delphi II[38] by solving the Poisson–Boltzmann equation[39-41]. In Delphi calculations, the grid spacing was assumed to 0.5 Å. Also, the radii of atoms were considered from the PARSE parameter set[42]. Internal and external dielectric constant values 2 and 80, respectively.

III. RESULTS AND DISCUSSION

A. Stability of the Protease - aptamer Complexes

Figure. 4 shows the root mean square deviation (RMSD) of the enzyme and aptamers in the complex during MD simulations time (150 ns). Talking about enzyme changes is more important

than aptamer, but comparing it with aptamer changes can be helpful. We expect that during the simulation of aptamer as an inhibitory drug, it may disrupt the structure or function of the protease enzyme, which can be explained by the more significant fluctuations that occur after drug interaction. Thus, it removes the enzyme from its natural state.

Figures show that the aptamer has a significant fluctuation, but unlike the aptamer, the enzyme has small fluctuations. As can be seen in the simulation path from the start to the end of the simulation time at 150 ns by the VMD graphics program, it can be stated that the aptamer changed a lot and its torsions were sometimes opened were and sometimes closed. It has been separated from the enzyme many times, but the enzyme has changed very little. The interaction of the enzyme and aptamer is stabilized in the 23305 frame (116 ns), and the interacting regions in the enzyme and the aptamer are detectable. However, conformational changes are still present, the enzyme is pre-separated from the 29527 (145 ns) frame, and it appears. Again from the 29527 frame (147 ns), the enzyme is separated from the aptamer, and it seems that this process is continuing, and the aptamer is unable to interact with the enzyme stably. Thus it can be concluded that the enzyme is less affected by AP1 and, its natural structure remains stable.

In complex 2, the residues involved in the interaction between the enzyme and the aptamer are detectable in the frame of 18784 (93ns). As shown in the figure, the fluctuations of the enzyme and aptamer still change in opposite ways. Thus, wherever the RMSD value in the aptamer is high, its value is downward for the enzyme, which could be the result of suitable interaction between them. As can be seen from the simulation pathway, the 16000 to 17000 frames (80 ns to 85 ns) correspond to the moments, when the drug is approaching the enzyme, and the 24000 to 25000 frames (120 ns to125 ns) correspond to the opening of portions of the enzyme involved with the aptamer and changed its structure from its original state. The graph shows that the fluctuations in the enzyme have increased from this moment to the last moment. Thus, it can be said that the

enzyme has been significantly affected by aptamer 2 and altered its conformation structure. On the other hand, aptamer has also changed due to this disorder. As you can see in the figure, the structure of the enzyme is partially closed and by the last moment, the flap is pulled down the active site. This is the case for the protease enzyme which means that after the formation of dimers there is no condition for the ligand to enter the active site anymore, thus impairing the function of the enzyme.

In the case of complex 3, their binding site was stabilized at a longer time than in the other two complexes, meaning that the aptamer was able to affect the enzyme after many times. This is after about two-thirds of the simulation time in the frame of 26310 (131 ns). The times before this time are related to the enzyme shift around the aptamer. For example, there are oscillations in frames 17000 to 22000. After the interaction, there is not much change in aptamer. The enzyme has also changed in the flap and dimer portion of the binding region. The flap section was downward until the simulation was completed and the enzyme form was partially closed, but in the final moments, it semi-opened slightly although the dimer section was upward and this was different from the initial state. This makes it difficult to access the binding site of the protease enzyme. In addition, after the binding time, the oscillations in the enzyme decreased and approached equilibrium, which is different from the enzyme diagram in complex 2 and it can be justified that probably complex diagram 2 and interaction process have better results for enzyme dysfunction. Another difference between complex 2 and 3 is that the average amount of remodeling for the enzyme in complex 2 is less than the other two complexes, indicating it has lost its stability and natural state. This is due to the fact that the amount of the root mean square deviation average for the free enzyme in the previous experiments is about 3.5 angstrom, which is about 2.39 angstrom for complex 2. Another evidence, is that aptamer 2 was able to stabilize the interaction faster than the other two aptamers. This indicates that aptamer 2 is more susceptible to enzyme inhibition. This result is consistent

with the experimental result[28].

B. Flexibility of the Protease – aptamer Complexes

In this analysis, we intend to examine the residues involved in the interaction of aptamer and enzyme as well as inhibition and disruption of the enzyme. To this end, we obtained RMSF analysis for the enzyme and aptamer in the complex in the pre-interaction and post-interaction frames. So that, we can compare the pre- and post-interacting residues and identify the stable residues. A brief look at the post-interaction graphs (Figure. 6) and their average values, as we expected and was revealed in the RMSD analyzes, aptamer and enzyme belonging to complex 2 have the highest values. RMSF averages indicate that they are more flexible than the other two complexes. This greater flexibility at the time after the interaction indicates that the enzyme is more affected by aptamer 2 and has been able to inhibit more than other aptamers. Therefore, AP2 is a better inhibitor. Whereas the mean RMSF was small for complex 3 and RMSD was close to the normal state of the enzyme. As such, it is less inhibitory but has a better affinity. This result is consistent with the experimental result for these aptamers[28]. On the other hand, a comparison between enzyme and aptamer structures before the interaction (Figure. 5) and the post-interaction state (Figure. 6) show that the residues involved in the interaction have less freedom than the pre-interaction state, will certainly have less flexibility and average RMSF value, which it is consistent with the results of previous work. This is also true for each of the residues before and after the interaction[43].

We now look at residues that have been affected or whose RMSFs have decreased or increased. As, can be seen in the (Table I, II and Figure. 7). In the case of complex 1, residues (35-41) that belong to the flap-elbow portion of the enzyme have the lowest RMSF, especially in residues 38 that corresponds to the Leucine in the enzyme. This is the area that has been involved in the

interaction with the aptamer, which in this area has less dynamic oscillations and movements, and the interaction has been well-formed. However, the flap-elbow region may play an important role in the function of the protease enzyme in interacting with the ligand, this reduction in flexibility relative to other enzyme residues may not be appropriate. Previous studies on the protease enzyme have emphasized the flexibility of this region, which is one of the key areas of inhibition. Another important area that may be involved in enzyme inhibition[44-46] is the flap-tip region of residues (54-46) which, unlike expected, has little flexibility in this complex. These results, according to the RMSD diagram, indicate that the enzyme is less affected. Therefore, the flexibility of these regions is reduced after the interaction and the enzyme maintains its natural state to a great extent. However, the mobility and hardening of these residues have caused to close the flap and to some extent prevent the ligand from entering the active site.

In complex 2, portions of the enzyme that interacted with aptamer 2 include the β-hairpin flap residues (47-41) and fragments of the flap-elbow. As expected, these regions are more flexible and suggest that aptamer-2 inhibition has occurred well in these regions, especially in proline 44, and is in agreement with previous experimental and theoretical results[44-46]. In addition, the residues 10, 21, 32, 43, 54, 65, 76 and 97, which belong to the fulcrum, flap, cantilever, dimer-interface, and C-terminal regions, are also highly flexible. The area around the active site, which contains residues (27-30), in particular, aspartic acid (25), has the least flexibility and exhibits a rigid behavior. This is also the case in previous works. On the other hand, residues 6 and 7 near the N-terminal region show little flexibility fluctuations, whereas in the (85-89) region this mobility is greater. In addition, a residue (15-21), which is the outer part of the fulcrum, is more flexible than the flap-elbow. This area probably acts as a lever for closing the flap. On the other hand, the flexibility in the dimer-interface segment (98-85) is the main autocatalysis site, it disrupts protein catalysis. In

general, it is conceivable that aptamer 2 acts as an allosteric inhibitor that alters enzyme conformation through greater flexibility of the flaps and elsewhere.

In complex 3, the inner part of the enzyme interacts with aptamer 3. These include the flap-tip area containing residues (53-47) and the dimer-interface containing residues (1-4). Unlike complex 2, the interacting residues in this complex had a lower RMSF value, indicating that aptamer 3 was less able to inhibit the residues involved than aptamer 2. But on the other hand, we can say that there is a better bond between them which is due to the better affinity of this aptamer and so these areas have been rigid. Higher affinity is also confirmed by RMSD analysis and ΔG calculation. But it seems that high affinity in these regions, especially in the dimer-interface, can be a an excellent barrier to dimer formation, which could be a an excellent anti-dimer inhibitor as described in the previous work by Yaakov Levy et al.[19] and the advantage is mentioned and according to studies by Duclair et al.[28] both are important areas in this aptamer which can interact. Since 75% of the homodimer stability is related to this part, Disruption in this area causes low performance. On the other hand, the RMSF values indicate low-mobility residues are more likely than high-mobility residues. However, previous work has shown that inhibitory residues can be both more flexible residues and hardened residues[45].

Of course, as noted in previous works, the areas around aspartic acid 25 as a triple active site region include residues (25-30 and 33), as well as portions of the flap (44-47, 49-52, 55) and cantilever regions (73-66) and residues (82-88) of the end-domain of the enzyme have low flexibility while the number of regions with high flexibility is limited, including 97 related to the dimer-interface and 62 and 66 of the final flap and the C-terminal terminus contains (90-97).

Although it is important to discuss RMSF values in the enzyme, a look at aptamer RMSF values can also be useful. These values are listed in the above table. The RMSF values of aptamer have the lowest values in the interaction regions, indicating that the relevant drug has less

flexibility in the interaction to obtain the appropriate interaction. These regions in aptamer 1and 3 include residues (33–29) and (32) of the stem-loop region, respectively. In the case of aptamer 2, the asymmetric interior loop region contains the residues (32-34). These areas with less flexibility are consistent with experimental results. The aptamer end residues in regions 3′ and 5′ did not play a role in binding, but the last 17 residues of region 3′ increased the affinity[28].

C. Radius of gyration of protease (Rg)

The radius of gyration used to describe the equilibrium conformation and the compactness of a macromolecule, especially bio macromolecules with the help of,

$$R_g = \sqrt{\frac{\sum_{i=1}^{N}(r_i - r_{cm})^2}{N}} \qquad (9)$$

Where r_i and r_{cm} are the coordinates of atom i and the center of the mass of N-atoms macromolecule with the assumption of the equal mass for all non-hydrogen atoms[47]. Changes in the gyration radius of a protein during a simulation pathway are a criterion for explaining its structural changes such as folding, expanding stretching and so on. In order to the investigation of effect aptamer on enzyme spatial form and its inhibition, Rg analysis calculated for single and complexed form for the last 5 ns of MD simulation. These values showed in Figure 8. As, it observed in Figure 8, Rg has the highest value for protease enzyme in complex 2 and since the protease in the monomeric state that we have chosen has been folded and stable[20] but its unfolded is unstable, then it can be concluded that enzyme in complex 2 affected more than other complexes by aptamer and changed its conformation. Furthermore, we obtained this analysis for all time simulation before and after frames of interaction (Figure. 9). It was the agreement with RMSD

analysis. Therefore fluctuating time in RMSD is similar to enhancement of Rg in these times. This indicates that compactness is less in these times and enzyme folding rates are accelerated. This process viewed in interaction start and after that, especially.

In complex 2, involved parts including flap-tip and flap-elbow that flap-tip is considered to be essential to enzyme function and after the simulation time the flap is pulled in toward the bottom of the active site (‘‘closed’’ form), whereas for the unbound enzyme all adopt a ‘‘semi-open’’ conformation with the flaps shifted away from the catalytic triads but still substantially closed over the active site and in contact with each other. Beside dimer-interface part pulled toward out and opened. It appears that the fully open state of the protease in dimer-interface part and high amounts of RMSF in the flap region and increase their flexibility had been the main role for increasing Rg and changing of enzyme conformation. In complex 3, flap tip and dimer-interfaced involved in the interaction between enzyme and AP3, unlike complex 2 that has more compactness and dimer-interface part pulled toward to aptamer and unfolded its conformation. Also, the RMSF values in the flap-tip and dimer-interface section decreased compared to the other two complexes. Thus, the structure of the enzyme remains folded and stable. In the case of complex 1, the interaction site is related to the outer portion of the protease enzyme and there are fewer changes to the dimer-interface section. Sometimes, it is open form and other times it is closed form. Therefore, aptamer 2 causes the highest values of Rg that has lost its natural compactness. This decrease in compactness can affect the contents of the secondary structure of the protease enzyme, which we discuss in DSSP analysis. In the RMSF analysis, we also discussed the most flexible residues that reduce the protease enzyme structure compactness.

D. Secondary structure of protease by DSSP analysis

DSSP is a program that is described by hydrogen bond and geometric model realization for

secondary structure assignment. Here, change of secondary structure is calculated during the last 5 ns[48]. Indeed, DSSP is the standard hydrogen-bond definition for the secondary structure. Also, it is a purely electrostatic model. The α-helix is shown in purple, the beta-sheet in yellow and the H bond turn in cyan (Figure.10) Before simulation, in Secondary Structure (DSSP) of this enzyme (1hhp), there was 48% beta-sheet (7 strands; 48 residues), 7% helical (1 helices; 7 residues including 4 (α-helix) and 3 (310 -helix)), 22% turn (22 residues and 6 turn) and 22% coil (22 residues and 5 coil). We calculated the contents of different secondary structures of HIV-1 PR in three complexes and compared it with the free state of the enzyme (Table. III). In all complexes, helix content remains constant. Since the α-helices tendency to consistently fold and unfold, it has been suggested that the 310-helix works as an intermediary confirmation of kinds, and presents insight into the initiation of α-helix folding. Therefore, the 310-helix was rapidly converted to α-helix during simulation time. However, at the end of the simulation, this content reached a fixed value for all three complexes.

In the case of complex 2, the results of previous analyses showed that aptamer 2, as an allosteric inhibitor, affects the protease enzyme. But in its secondary structure, aptamer 2 appears to increase turn content and increase coil content, while the content of beta-sheet and helix remained constant. It is conjectured that this change was due to the decrease in the protease structure compactness that we obtained from Rg analysis and the greater flexibility that came from RMSF analysis. In complex 3, where aptamer 3 had the highest affinity for the interaction with the protease, the beta-sheet and turn content increased the most, while the coil content decreased the most. This indicates that the secondary structure of the enzyme was most stable after the interaction. This result is in agreement with the results in Rg, RMSF and RMSD analysis.

D. Hydrogen bonds (HB)

The normalized distribution of the hydrogen bonds was examined by Gaussian-type interactions[49]. In this equation, the average number of hydrogen bonds (μ) and the standard deviation (σ), was measured through the fitting of the Eq. (2) as a result, we can obtain the distribution data.

$$f(x) = \frac{a}{\sigma.\sqrt{2\pi}} \exp \frac{-(\mu-\bar{\mu})^2}{2.\sigma^2} \qquad (11)$$

This analysis is shown that the condition of waters near the protease and aptamers would be affected by the interaction between water and each of them. (See Table IV. and Fig. 11) has been contained the average number of hydrogen bonds of water-aptamer hydrogen bonds singly and complexed with protease in a thin layer immediate the aptamer. This average value shows that the interaction of protease with the aptamer slightly increases the water-aptamer hydrogen bonds. The enhancement of the number of hydrogen bonds resulted from the attractive hydrophilic interaction between the aptamers and the water molecules. This enhancement is more for AP2. Then aptamer 2 interact with the enzyme from the hydrophobic domain and have given their hydrophilic parts to the water molecules.

Also, Table 4 been contained a comparison of the average number of water-protease hydrogen bonds for the water-PR system singly and complexed with aptamer. These average values show that the interaction of protease with the aptamer slightly increases the hydrogen bonds near the protease in complex 2 than other complexes. This indicates that the protease in complex 2 interacted with aptamer by the hydrophobic parts and provided the hydrophilic regions for water molecules, unlike complex 3 that the protease from hydrophobic parts interacted with the waters, and reduced the hydrogen bonds with the surrounding water. On the other hand, by looking at the secondary structure of the protease enzyme and the parts that have been identified to interact with aptamer 2, it can be seen that the sections of the protease include flap tip and flap-elbow by

hydrophobic residues including residues (41-47) interact with aptamer better of the hydrophilic parts of the enzyme. This shows that electrostatic interaction between AP2 and enzyme is less than the other two complexes while in complex 3, the amount of electrostatic energy was the highest. Increasing electrostatic energy reduces the hydrophobic property of the interaction between the aptamer 3 and the enzyme in the complex. This hypothesis proved by ΔG calculation.

Analysis of the hydrogen bond between aptamer and protease indicates that there is less water between the two components, especially in complex 3. This is an average of about 0.147. You can see the position of the waters in Figure 12. A critical point about the waters between protease and aptamer 3 is that the water in this part has become a chain and oxygen and hydrogen atoms have a particular order that is visible in this frame and before frames. Therefore, interaction in this complex is made easier due to fewer space constraints. Because of the high electrostatic energy between them, it can be concluded that aptamer 3 has a higher affinity. This hypothesis proved by ΔG calculation.

F. Free energy calculations by MM-PBSA method

Table. V shows the average of the binding free energies and their corresponding components in the complexes at 310 K. These parameters obtained from the MM-PBSA calculation for three complexes. In complex 3, the total binding energy was negative with the highest value but in complex 2 was the least value that leads to a spontaneous process. This is in agreement with hydrogen bond analysis. In fact, according to previous experimental studies[28, 35] and structural reasons related to a mutation in AP3, we expected this interaction for aptamer 3 which has increased its compound affinity.

The corresponding components of the average binding energy $\Delta G_{binding}$, were calculated for three complexes. The results in table 5 showed that, ΔG_{pb} and ΔG_{npb} were unfavorable but ΔE_{MM} was

favorable for the formation of the enzyme-aptamer complexes. Since the interaction between the enzyme and the aptamer is non-bonded, the bonded terms do not play a role in interaction. Therefore, only both van der Waals and electrostatic terms are included in ΔE_{MM}.

Additionally, to identify which type of interactions plays the main role in the enzyme blocking, we calculated the van der Waals, electrostatic between the HIV-1 PR and aptamers using the NAMD energy plugin of VMD [27,30], (Table. VI) for the interaction of enzyme with the studied aptamers along the last 5 ns simulation run time. Overall, these results showed the positive contribution of electrostatic interaction and the negative contribution of van der Waals interaction in the studied simulation. In other words, the contribution of van der Waals interactions in the total interaction energy was smaller than the electrostatic energy. Thus, according to the results of the two ways, we can be stated that electrostatic interactions have essential roles in the formation of the complex. As was observed in the hydrogen bond analysis, the amount of electrostatic energy for complex 3 was greater than in other complexes. This value in complex 2 was the lowest. Another reason for confirming electrostatic interactions is that aptamers have a negatively partial charge and protease enzyme has a positive partial charge. Protease enzyme surface charge analysis in previous studies[50] shows that positively charged residues that would form more favorable interactions with the aptamers. In complex 3 these residues are in the flaps section.

IV. CONCLUSION

The structural results of the simulation related to RMSD, RMSF, DSSP, Rg, and hydrogen bond analysis as well as energetic results including the binding energy and the contribution of van der Waals and electrostatic interaction energy in it have been extracted and discussed. The structural results show that the aptamers interacted with the enzyme and we found that aptamer 2 is a better inhibitor and a potential allosteric inhibitor that changes the protease enzyme conformation. In

addition to the above results, the energetic result reveals that aptamer 3 has a relatively high affinity to their target by interacting with the dimer-interface part; it disrupts the structural stability and impedes dimer formation, thus disrupting the function of the enzyme. Finally, with due attention to the high effectiveness and the proprietary function of aptamers, we can conclude that these compounds may be considered as effective HIV-1 anti-protease drugs. Our work reveals details about how aptamers inhibit HIV-1 PR. The results will be helpful for the further design and discovery of new inhibitors.

ACKNOWLEDGMENTS

This work has been supported by Azarbaijan Shahid Madani University. [Grant number 214/D/25972].

REFERENCES

[1] Walsh JC, Jones CD, Barnes EA, Gazzard BG, Mitchell SM. Increasing survival in AIDS patients with cytomegalovirus retinitis treated with combination antiretroviral therapy including HIV protease inhibitors. Aids. 1998 Apr 16;12(6):613-8.

[2] Lee CA, Kessler CM, Varon D, Martinowitz U, Heim M, Condra JH. Resistance to HIV protease inhibitors. Haemophilia: State of the Art. 1998 Jul;4(4):610-5.

[3] Ellington AD, Szostak JW. In vitro selection of RNA molecules that bind specific ligands. nature. 1990 Aug;346(6287):818.

[4] Bock LC, Griffin LC, Latham JA, Vermaas EH, Toole JJ. Selection of single-stranded DNA molecules that bind and inhibit human thrombin. Nature. 1992 Feb;355(6360):564.

[5] Ellington AD. RNA selection: Aptamers achieve the desired recognition. Current Biology. 1994 May 1;4(5):427-9.

[6] Famulok M. Oligonucleotide aptamers that recognize small molecules. Current opinion in structural biology. 1999 Jun 1;9(3):324-9.

[7] Famulok M, Mayer G, Blind M. Nucleic acid aptamers from selection in vitro to applications in vivo. Accounts of Chemical research. 2000 Sep 19;33(9):591-9.

[8] Radom F, Jurek PM, Mazurek MP, Otlewski J, Jeleń F. Aptamers: molecules of great potential. Biotechnology advances. 2013 Dec 1;31(8):1260-74.

[9] Hermann T, Patel DJ. Adaptive recognition by nucleic acid aptamers. Science. 2000 Feb 4;287(5454):820-5.

[10] Hermann T, Patel DJ. RNA bulges as architectural and recognition motifs. Structure. 2000 Mar 1;8(3):R47-54.

[11] Stoltenburg R, Strehlitz B. Refining the results of a classical SELEX experiment by expanding the sequence data set of an aptamer pool selected for Protein A. International journal of molecular sciences. 2018 Feb 24;19(2):642.

[12] Tuerk C, Gold L. Systematic evolution of ligands by exponential enrichment: RNA ligands to bacteriophage T4 DNA polymerase. science. 1990 Aug 3;249(4968):505-10.

[13] Lin PH, Kao YH, Chang Y, Cheng YC, Chien CC, Chen WY. Daunomycin interaction with DNA: microcalorimetric studies of the thermodynamics and binding mechanism. Biotechnology journal. 2010 Oct;5(10):1069-77.

[14] Zutshi R, Franciskovich J, Shultz M, Schweitzer B, Bishop P, Wilson M, Chmielewski J. Targeting the dimerization interface of HIV-1 protease: inhibition with cross-linked interfacial peptides. Journal of the American Chemical Society. 1997 May 28;119(21):4841-5.

[15] Bowman MJ, Chmielewski J. Novel strategies for targeting the dimerization interface of HIV protease with cross-linked interfacial peptides. Peptide Science: Original Research on Biomolecules. 2002;66(2):126-33.

[16] Boggetto N, Reboud-Ravaux M. Dimerization inhibitors of HIV-1 protease. Biological chemistry. 2002 Sep 17;383(9):1321-4.

[17] Caflisch A, Schramm HJ, Karplus M. Design of dimerization inhibitors of HIV-1 aspartic proteinase: a computer-based combinatorial approach. Journal of computer-aided molecular design. 2000 Feb 1;14(2):161-79.

[18] Levy Y, Caflisch A. Flexibility of monomeric and dimeric HIV-1 protease. The Journal of Physical Chemistry B. 2003 Apr 3;107(13):3068-79.

[19] Levy Y, Caflisch A, Onuchic JN, Wolynes PG. The folding and dimerization of HIV-1 protease: evidence for a stable monomer from simulations. Journal of molecular biology. 2004 Jun 25;340(1):67-79.

[20] Eisold A, Labudde D. Detailed Analysis of 17β-Estradiol-Aptamer Interactions: A Molecular Dynamics Simulation Study. Molecules. 2018 Jul;23(7):1690.

[21] Kalé L, Skeel R, Bhandarkar M, Brunner R, Gursoy A, Krawetz N, Phillips J, Shinozaki A, Varadarajan K, Schulten K. NAMD2: greater scalability for parallel molecular dynamics. Journal of Computational Physics. 1999 May 1;151(1):283-312.

[22] Feller SE, MacKerell AD. An improved empirical potential energy function for molecular simulations of phospholipids. The Journal of Physical Chemistry B. 2000 Aug 10;104(31):7510-5.

[23] Brooks BR, Bruccoleri RE, Olafson BD, States DJ, Swaminathan SA, Karplus M. CHARMM: a program for macromolecular energy, minimization, and dynamics calculations. Journal of computational chemistry. 1983 Jun;4(2):187-217.

[24] MacKerell Jr AD, Bashford D, Bellott ML, Dunbrack Jr RL, Evanseck JD, Field MJ, Fischer S, Gao J, Guo H, Ha S, Joseph-McCarthy D. All-atom empirical potential for molecular modeling and dynamics studies of proteins. The journal of physical chemistry B. 1998 Apr 14;102(18):3586-616.

[25] Humphrey W, Dalke A, Schulten K. VMD: visual molecular dynamics. Journal of molecular graphics. 1996 Feb 1;14(1):33-8.

[26] Mark P, Nilsson L. Structure and dynamics of the TIP3P, SPC, and SPC/E water models at 298 K. The Journal of Physical Chemistry A. 2001 Nov 1;105(43):9954-60.

[27] Spinelli S, Liu QZ, Alzari PM, Hirel PH, Poljak RJ. The three-dimensional structure of the aspartyl protease from the HIV-1 isolate BRU. Biochimie. 1991 Nov 1;73(11):1391-6.

[28] Duclair S, Gautam A, Ellington A, Prasad VR. High-affinity RNA aptamers against the HIV-1 protease inhibit both in vitro protease activity and late events of viral replication. Molecular Therapy-Nucleic Acids. 2015 Jan 1;4:e228.

[29] Xayaphoummine A, Bucher T, Isambert H. Kinefold web server for RNA/DNA folding path and structure prediction including pseudoknots and knots. Nucleic acids research. 2005 Jul 1;33(suppl_2):W605-10.

[30] Magnus M, Boniecki MJ, Dawson W, Bujnicki JM. SimRNAweb: a web server for RNA 3D structure modeling with optional restraints. Nucleic acids research. 2016 Apr 19;44(W1):W315-9.

[31] Xu L, Sun H, Li Y, Wang J, Hou T. Assessing the performance of MM/PBSA and MM/GBSA methods. 3. The impact of force fields and ligand charge models. The journal of physical chemistry B. 2013 Jul 8;117(28):8408-21.

[32] Sun H, Li Y, Tian S, Xu L, Hou T. Assessing the performance of MM/PBSA and MM/GBSA methods. 4. Accuracies of MM/PBSA and MM/GBSA methodologies evaluated by various simulation protocols using PDBbind data set. Physical Chemistry Chemical Physics. 2014;16(31):16719-29.

[33] Muzzioli E, Del Rio A, Rastelli G. Assessing Protein Kinase Selectivity with Molecular Dynamics and MM-PBSA Binding Free Energy Calculations. Chemical biology & drug design. 2011 Aug;78(2):252-9.

[34] Xu L, Li Y, Li L, Zhou S, Hou T. Understanding microscopic binding of macrophage migration inhibitory factor with phenolic hydrazones by molecular docking, molecular dynamics simulations and free energy calculations. Molecular BioSystems. 2012;8(9):2260-73.

[35] Chang S, Zhang DW, Xu L, Wan H, Hou TJ, Kong R. Exploring the molecular basis of RNA recognition by the dimeric RNA-binding protein via molecular simulation methods. RNA biology. 2016 Nov 1;13(11):1133-43.

[36] Homeyer N, Gohlke H. Free energy calculations by the molecular mechanics Poisson− Boltzmann surface area method. Molecular Informatics. 2012 Feb;31(2):114-22.

[37] Kumari R, Kumar R. C. Open Source Drug Discovery and A. Lynn. J. Chem. Inf. Model. 2014;54:1951-62.

[38] Gilson MK, Sharp KA, Honig BH. Calculating the electrostatic potential of molecules in solution: method and error assessment. Journal of computational chemistry. 1988 Jun;9(4):327-35.

[39] Baker NA, Sept D, Joseph S, Holst MJ, McCammon JA. Electrostatics of nanosystems: application to microtubules and the ribosome. Proceedings of the National Academy of Sciences. 2001 Aug 28;98(18):10037-41.

[40] Srinivasan J, Cheatham TE, Cieplak P, Kollman PA, Case DA. Continuum solvent studies of the stability of DNA, RNA, and phosphoramidate− DNA helices. Journal of the American Chemical Society. 1998 Sep 23;120(37):9401-9.

[41] Honig B, Nicholls A. Classical electrostatics in biology and chemistry. Science. 1995 May 26;268(5214):1144-9.

[42] Sitkoff D, Sharp KA, Honig B. Accurate calculation of hydration free energies using macroscopic solvent models. The Journal of Physical Chemistry. 1994 Feb;98(7):1978-88.

[43] Hou T, Yu R. Molecular dynamics and free energy studies on the wild-type and double mutant HIV-1 protease complexed with amprenavir and two amprenavir-related inhibitors: mechanism for binding and drug resistance. Journal of medicinal chemistry. 2007 Mar 22;50(6):1177-88.

[44] Ishima R, Freedberg DI, Wang YX, Louis JM, Torchia DA. Flap opening and dimer-interface flexibility in the free and inhibitor-bound HIV protease, and their implications for function. Structure. 1999 Sep 15;7(9):1047-S12.

[45] Zoete V, Michielin O, Karplus M. Relation between sequence and structure of HIV-1 protease inhibitor complexes: a model system for the analysis of protein flexibility. Journal of molecular biology. 2002 Jan 4;315(1):21-52.

[46] Freedberg DI, Wang YX, Stahl SJ, Kaufman JD, Wingfield PT, Kiso Y, Torchia DA. Flexibility and function in HIV protease: Dynamics of the HIV-1 protease bound to the asymmetric inhibitor kynostatin 272 (KNI-272). Journal of the American Chemical Society. 1998 Aug 12;120(31):7916-23.

[47] Lobanov MY, Bogatyreva NS, Galzitskaya OV. Radius of gyration as an indicator of protein structure compactness. Molecular Biology. 2008 Aug 1;42(4):623-8.

[48] Kabsch W, Sander C. Dictionary of protein secondary structure: pattern recognition of hydrogen-bonded and geometrical features. Biopolymers: Original Research on Biomolecules. 1983 Dec;22(12):2577-637.

[49] McQuarrie DA. Statistical thermodynamics. 1984.

[50] Huang L, Sayer JM, Swinford M, Louis JM, Chen C. Modulation of human immunodeficiency virus type 1 protease autoprocessing by charge properties of surface residue 69. Journal of virology. 2009 Aug 1;83(15):7789-93

Table I. The interacted residues with their average RMSF values in aptamer.

Region	Base Range in aptamer	RMSF [Å] before interaction	RMSF [Å] of after interaction
Stem-loop	A29 (AP1)	33.84	11.08
	G30 (AP1)	33.55	11.33
	G31 (AP1)	33.19	11.90
	C32 (AP1)	33.20	11.82
	U33 (AP1)	22.80	4.96
	U32 (AP3)	32.09	11.92
asymmetric interior loop	U32 (AP2)	34.72	21.69
	G33 (AP2)	38.10	18.34
	U34 (AP2)	33.84	19.46

Table II. The interacted residues with their average RMSF values in HIV-1 PR.

Region	Base Range in protease	RMSF [Å] of before interaction	RMSF [Å] of after interaction
	G35 (AP1)	26.84	12.86
	M36 (AP1)	26.75	12.72
	S37 (AP1)	26.72	12.64
Flap-elbow	L38(AP1)	26.81	12.58
	P39 (AP1)	26.81	12.77
	G40 (AP1)	26.93	12.95
	R41 (AP1)	26.98	13.46
β-hairpin flap	W42(AP2)	32.64	22.00
	K43(AP2)	32.37	21.89
	P44 (AP2)	32.93	24.20
	K45 (AP2)	32.02	21.32
	M46 (AP2)	32.98	21.20
Flap-tip	I47 (AP3)	33.50	4.98
	G48 (AP3)	33.55	5.19
	G49 (AP3)	33.80	4.96
	I50 (AP3)	34.12	4.77
	G51 (AP3)	34.53	4.82
	G52 (AP3)	35.25	4.87
	F53 (AP3)	35.84	5.25
Dimer interface	P1 (AP3)	39.32	5.48
	Q2 (AP3)	39.22	5.44
	I3 (AP3)	39.69	5.76
	T4 (AP3)	39.06	5.71

Table III. The averaged secondary structure contents of HIV-1 PR in different simulation systems. Data are calculated based on the last 5 ns of the simulation.

Secondary structures	β-sheet (%) (Extended strand)	Helix (%) (α-helix), (3_{10} -helix)	Turn (%)	Coil (%)
Free PR	47 residues and 7 strands: (47.47%)	7 residues and 1 helices: 7 (α-helix) (7.07%)	15 residues and 5 turn (15.15%)	30 residues and 7 coil (30.3%)
PR in complex 1	49 residues and 7 strands: (49.49%)	7 residues and 1 helices: 7 (α-helix) (7.07%)	6 residues and 3 turn: (6.06%)	37 residues and 5 coil: (37.37%)
PR in complex 2	47 residues and 6 strands: (47.47%)	7residues and 1 helices: 7 (α-helix) (7.07%)	18 residues and 5 turn: (18.18%)	27 residues and 7 coil: (27.27%)
PR in complex 3	51 residues and 6 strands: (51.52%)	7 residues and 1 helices: 7 (α-helix) (7.07%)	20 residues and 5 turn: (20.2%)	21 residues and 7 coil: (21.21%)

Table IV. Values of the average number of hydrogen bonds and the standard deviation of the distribution for AP1, AP2 and AP3 as single and complexed (A) and protein and water (B) containing systems of single and complexed for HIV-1 PR during the last 5ns of MD simulation.

System	Average number of hydrogen bonds in aptamers	Sigma (σ)
AP1	123.682 +/- 2.495	24.7764
AP2	101.664 +/- 0.5635	12.9623
AP3	102.36 +/- 2.013	17.8894
AP1 in Complex 1	131.576 +/- 0.7107	15.6602
AP2 in Complex 2	149.25 +/- 0.3898	13.8278
AP3 in Complex 3	148.883 +/- 0.1854	10.9871

System	Average number of hydrogen bonds in protease	Sigma (σ)
PR	59.8128 +/- 1.432	15.0392
PR in Complex 1	68.9009 +/- 0.4388	10.0567
PR in Complex 2	77.6879 +/- 0.1698	6.92453
PR in Complex 3	48.1174 +/- 0.1518	6.02031

TableV. The average binding energy of the AP-PR complex (Kcal/mol) during MD simulation. The molecular mechanic's potential energy (ΔE_{MM}), the polar solvation free energy (ΔG_{polar}), non-polar solvation free energy ($\Delta G_{nonpolar}$), and total binding energies ($\Delta G_{binding}$) are calculated using MM-PBSA method.

System	ΔE_{MM}	ΔG_{polar}	$\Delta G_{nonpolar}$	$\Delta G_{Binding}$
Complex- AP1	−1163.93	241.72	−8.00	−930.20
Complex- AP2	−440.63	283.82	−3.75	−160.55
Complex- AP3	−1192.45	97.67	−2.50	−1097.29

TableVI. The van der Waals and electrostatic energies and their contribution to the total interaction energy.

System	van der Waals energy (kcal.mol-1)	Electrostatic energy (kcal.mol-1)	Total energy (kcal.mol-1)
Complex-AP1	418.87	-1200.08	-781.21
Complex-AP2	-20.18	-437.97	-458.14
Complex-AP3	158.71	-1265.27	-1106.55

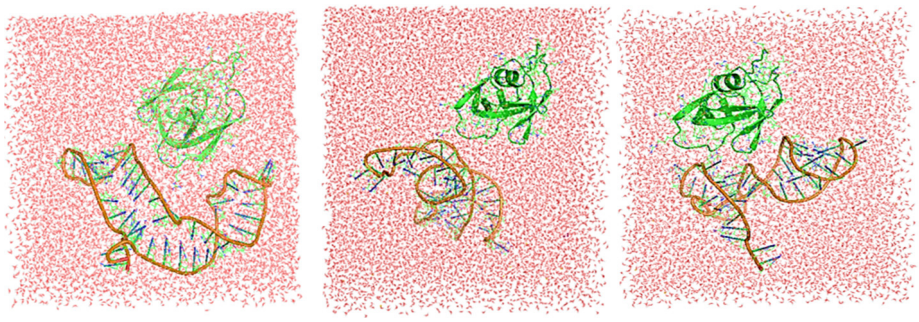

a b c

Figure 1. The molecular dynamics simulation box of aptamer and enzymes with water. (a) AP1 with the protease enzyme. (b) AP2 with the protease enzyme. (c) AP3 with the protease enzyme.

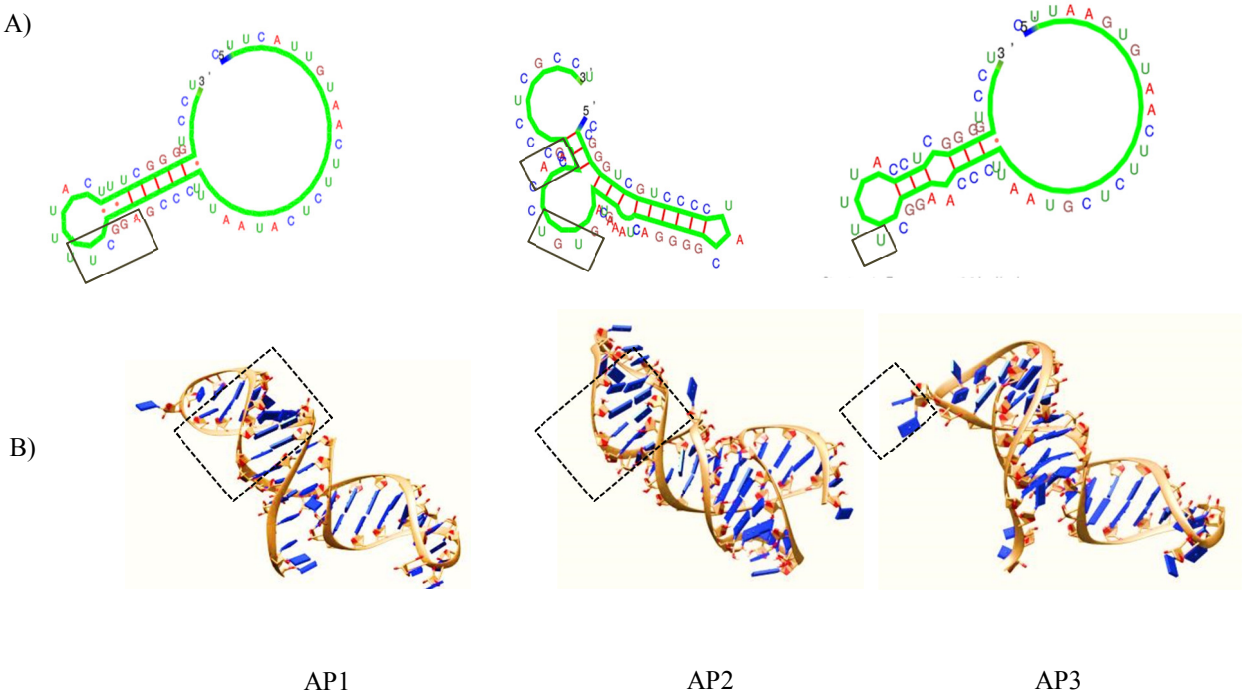

Figure 2. (**A**) 2D structure of the anti-HIV-1 PR RNA aptamer by kinefold. Bases Red lines form base pairs, and base dots in red are unpaired. (**B**) 3D structure of the anti-HIV-1 PR RNA aptamer obtained from SIMRNA. The regions identified are those that have interacted with the protease enzyme.

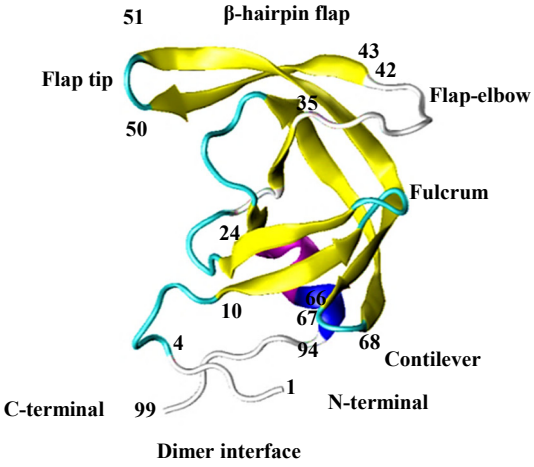

Figure 3. New Cartoon of the three-dimensional structure of the aspartyl protease from the HIV-1 PR: a)Extended beta, yellow; b) Turn, cyan; c)Alpha helix, purple; d)3-10 helix, blue; e)Coil, white. The figure was created from the 1HPP PDB file using VMD. Numbers indicate distinct regions. Flaps: residues 43–66; flap tips: residues 50–51; flap elbow: residues 35–42; cantilever: residues 67–68; fulcrum: residues 10–24; and the dimer interface: residues 1–4 and 94–99.

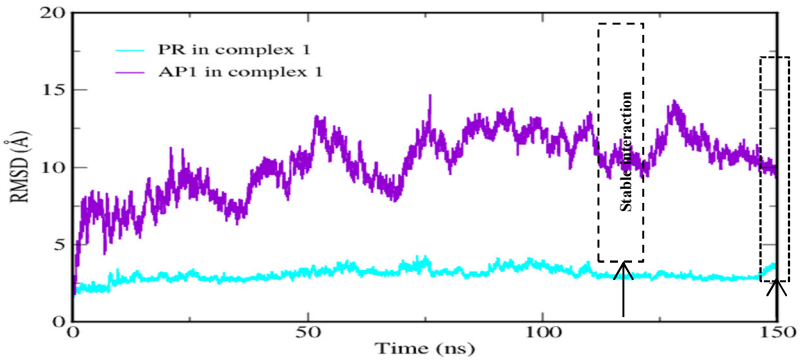

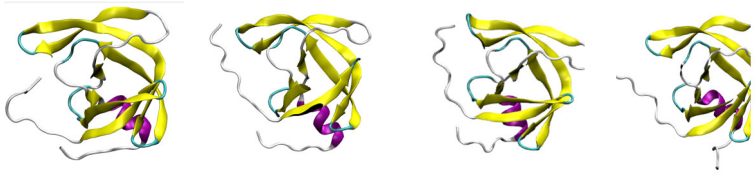

time = 0 ns
closed

time = 116 ns
closed

time = 147 ns
opened

time = 150 ns
closed

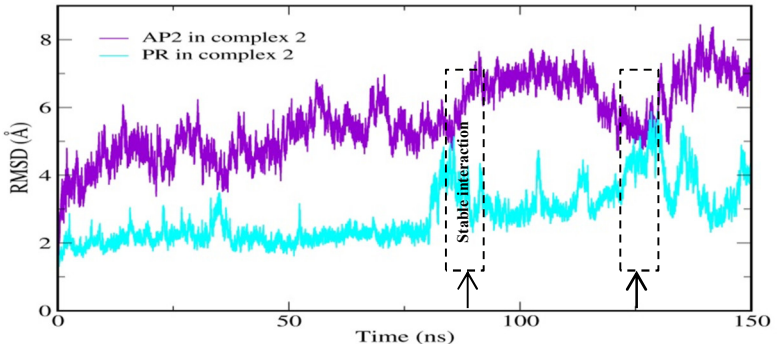

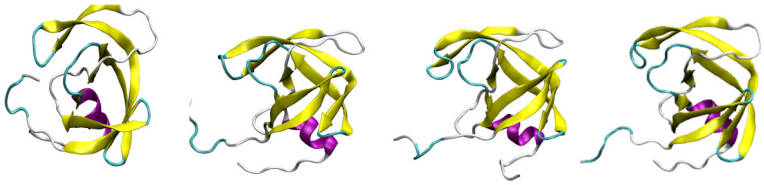

time = 0 ns
closed

time = 93 ns
closed

time = 121 ns
closed

time = 150 ns
closed

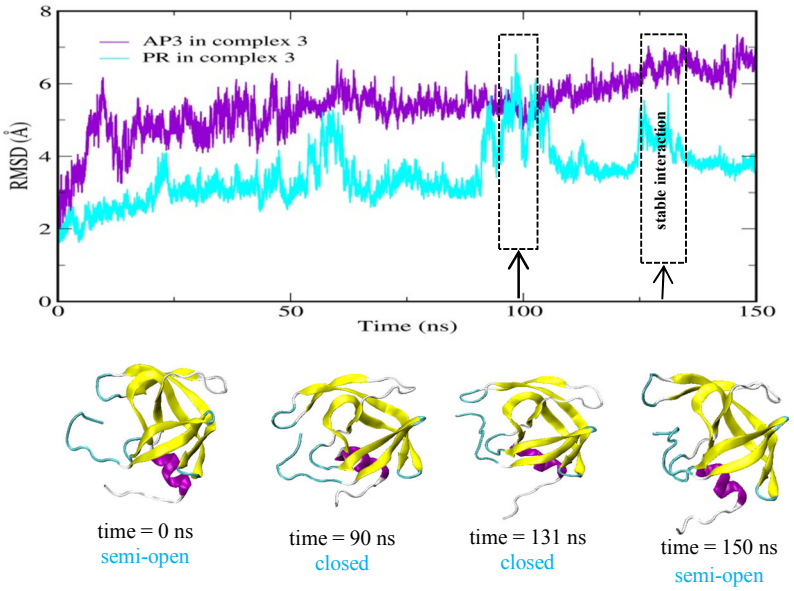

Figure 4. RMSD of aptamers and HIV-1 PR in the complex along the MD simulation time (150 ns).

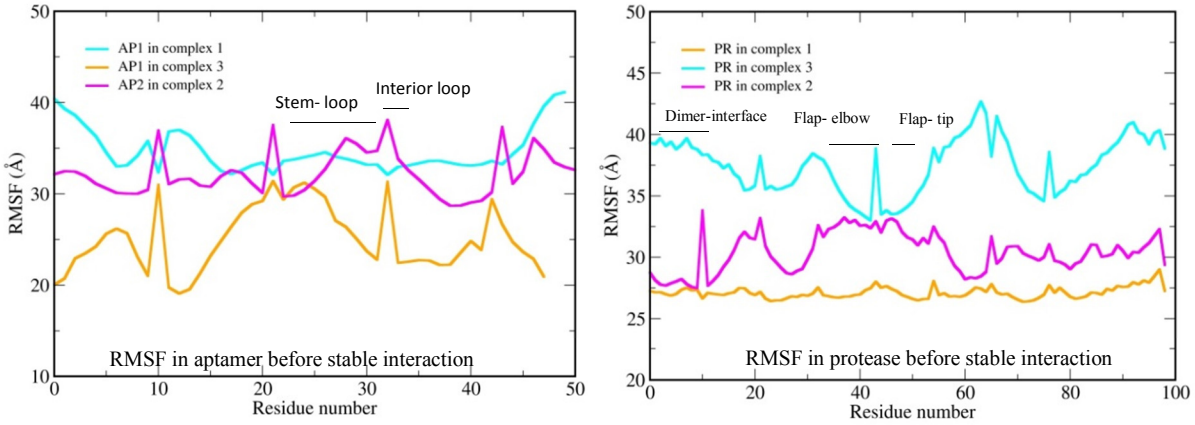

Figure 5. Calculated RMSF of complex vs. residue number for HIV-1 PR (99 residues) and aptamer AP1, AP2, AP3 (48, 50, 51 residues) during the MD simulation in before of stable interaction.

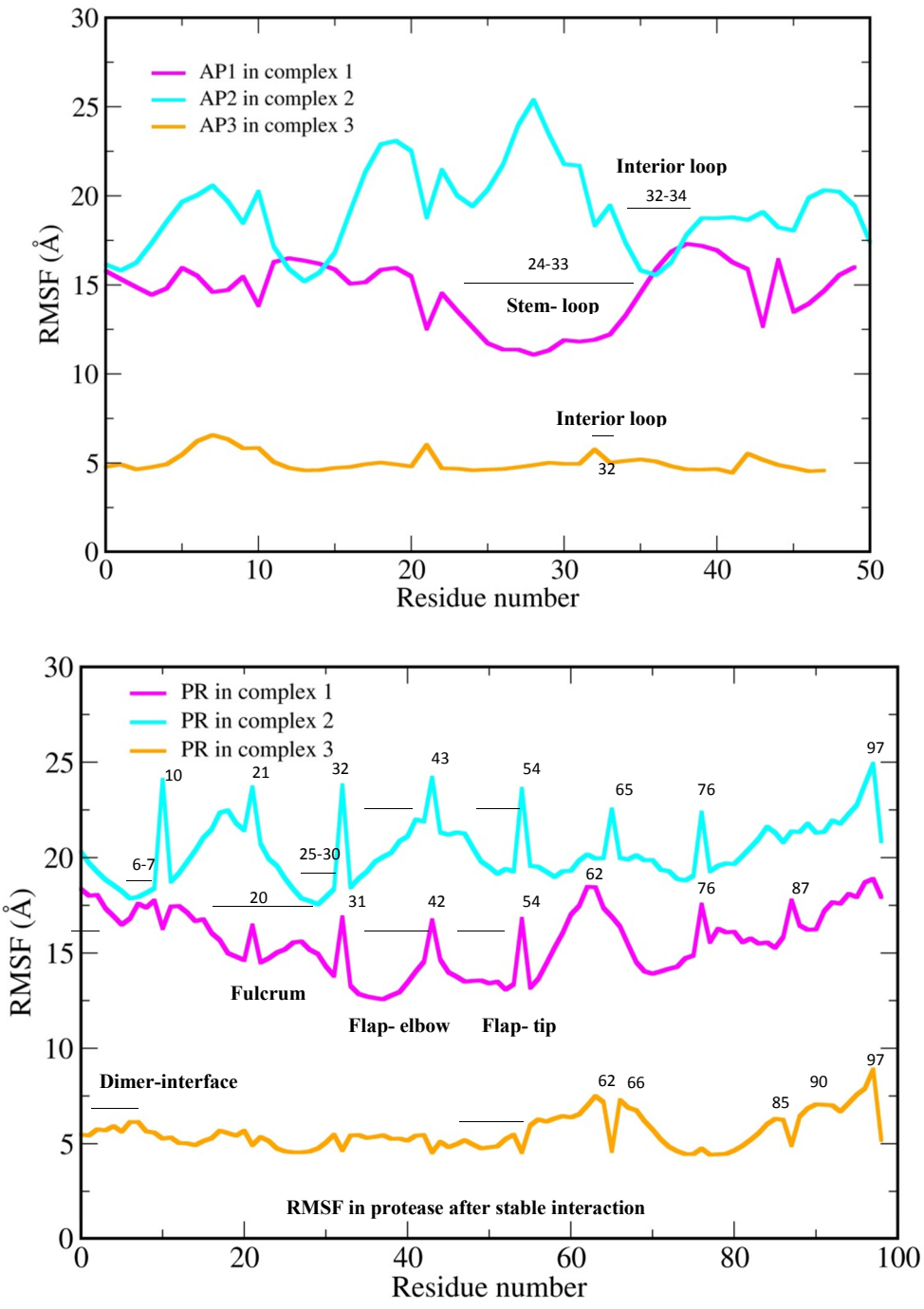

Figure6. Calculated RMSF of complex vs residue number for HIV-1 PR (99 residues) and aptamer AP1, AP2, AP3 (48, 50, 51 residues) during the MD simulation in after of stable interaction.

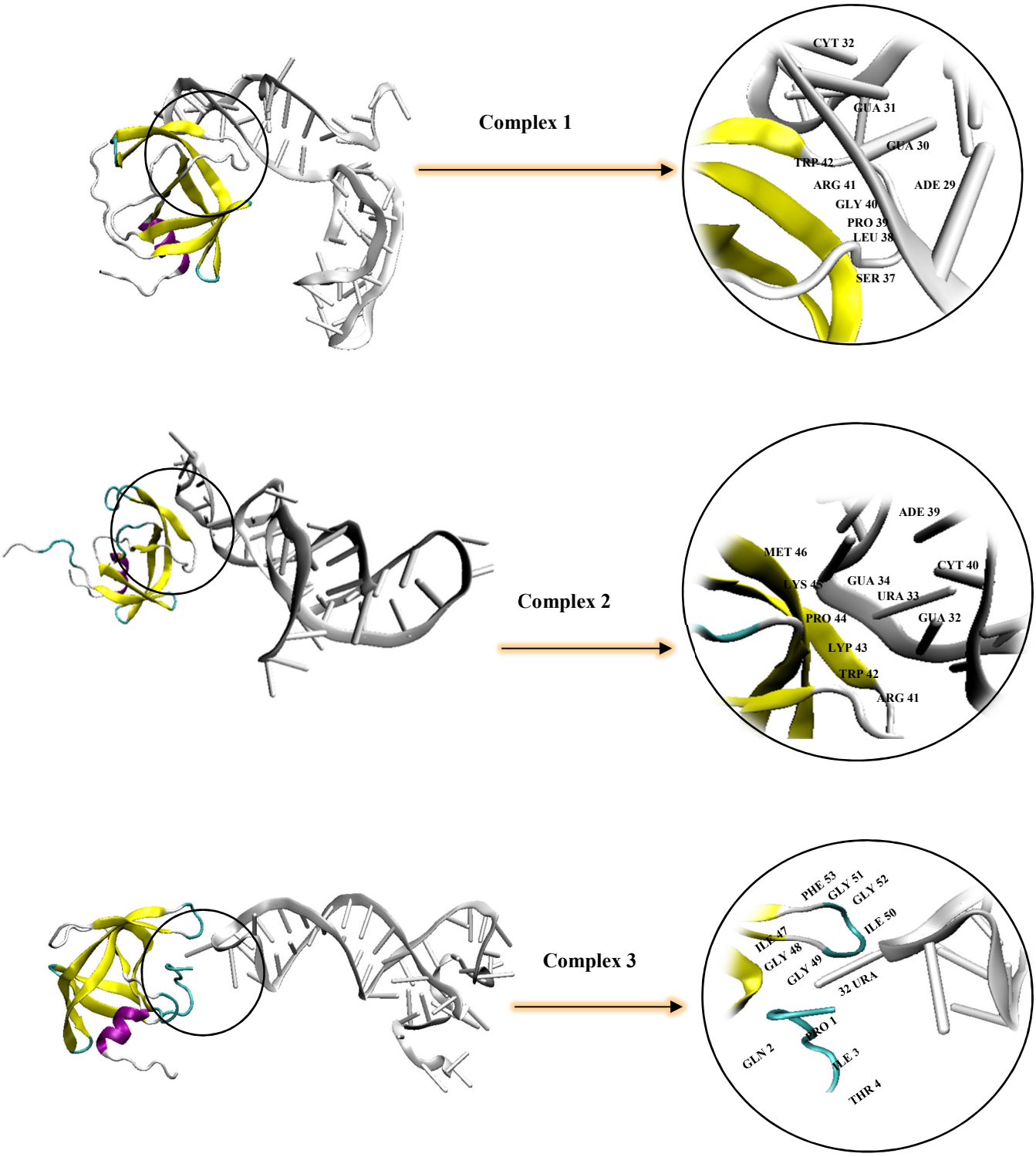

Figure 7. A snapshot of interaction between enzyme and AP1, AP2, and AP3 at the end of the simulation and the residues who have contributed to the interaction.

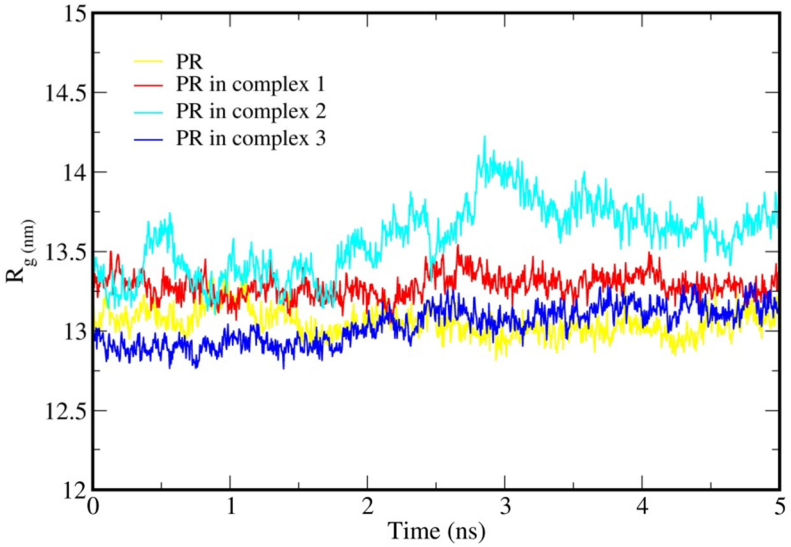

Figure 8. The *Rg* of HIV-1 PR in complex 1, 2 and 3 along the simulation time (last 5ns).

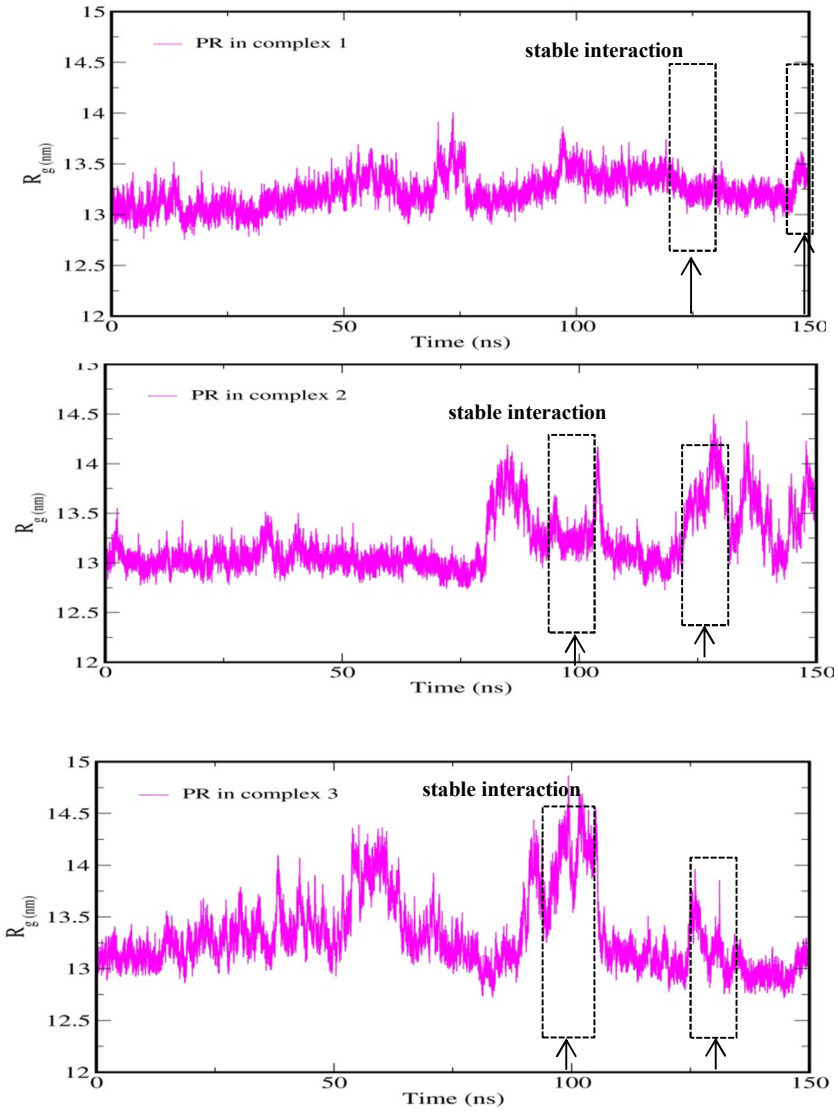

Figure 9. The *Rg* of HIV-1 PR in complex 1, 2 and 3 along the simulation time (150ns).

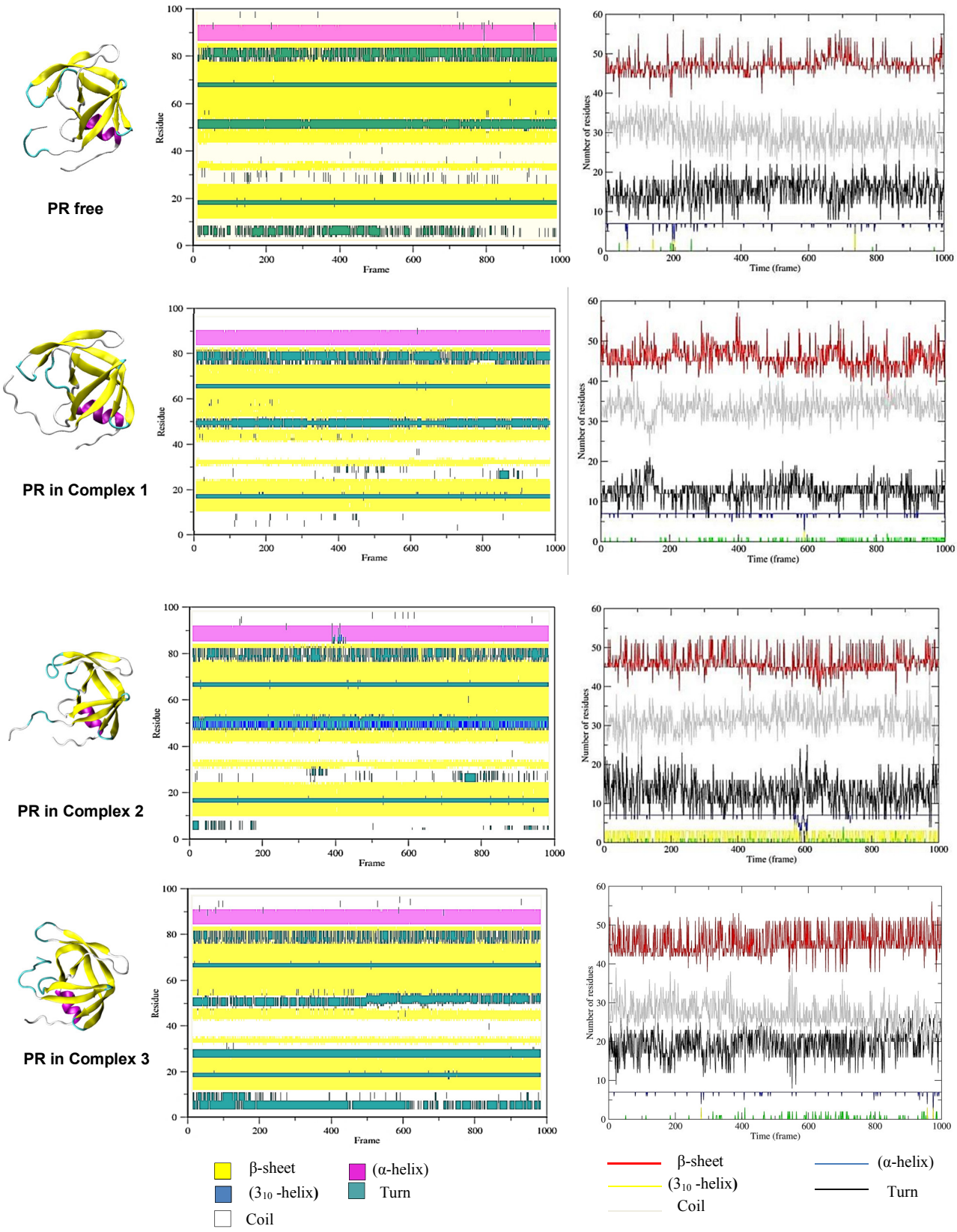
PR free
PR in Complex 1
PR in Complex 2
PR in Complex 3
Residue
Frame
Number of residues
Time (frame)
β-sheet
(α-helix)
(3₁₀ -helix)
Turn
Coil

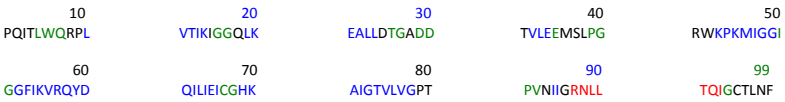

Figure 10. The DSSP analysis of secondary structure during the simulation (last 5ns) and the cartoon model of the last snapshot of MD for the enzyme structure in complex 1, 2 and 3 and free enzyme are shown in right, respectively.

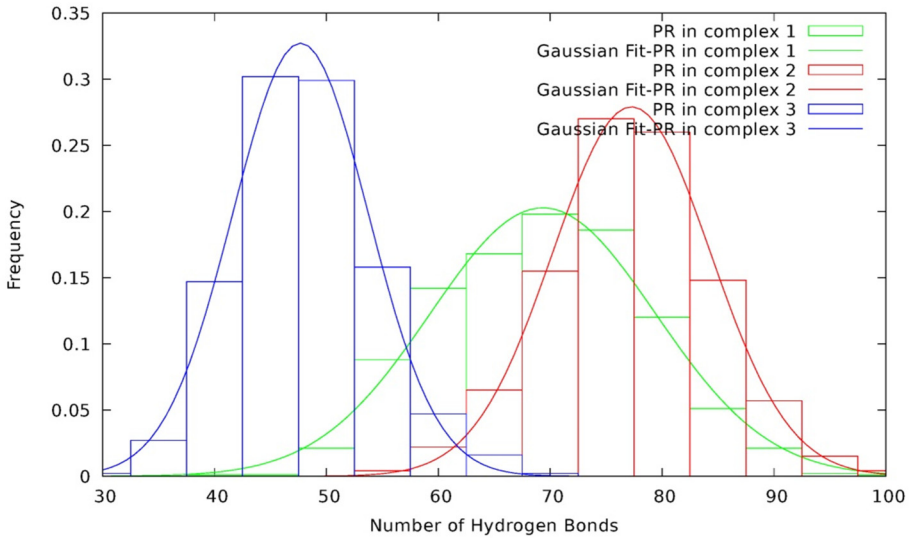

Figure 11. Distribution of the normalized number of hydrogen bonds of HIV-1 PR and water-containing systems of the complex during the last 5ns of MD simulation.

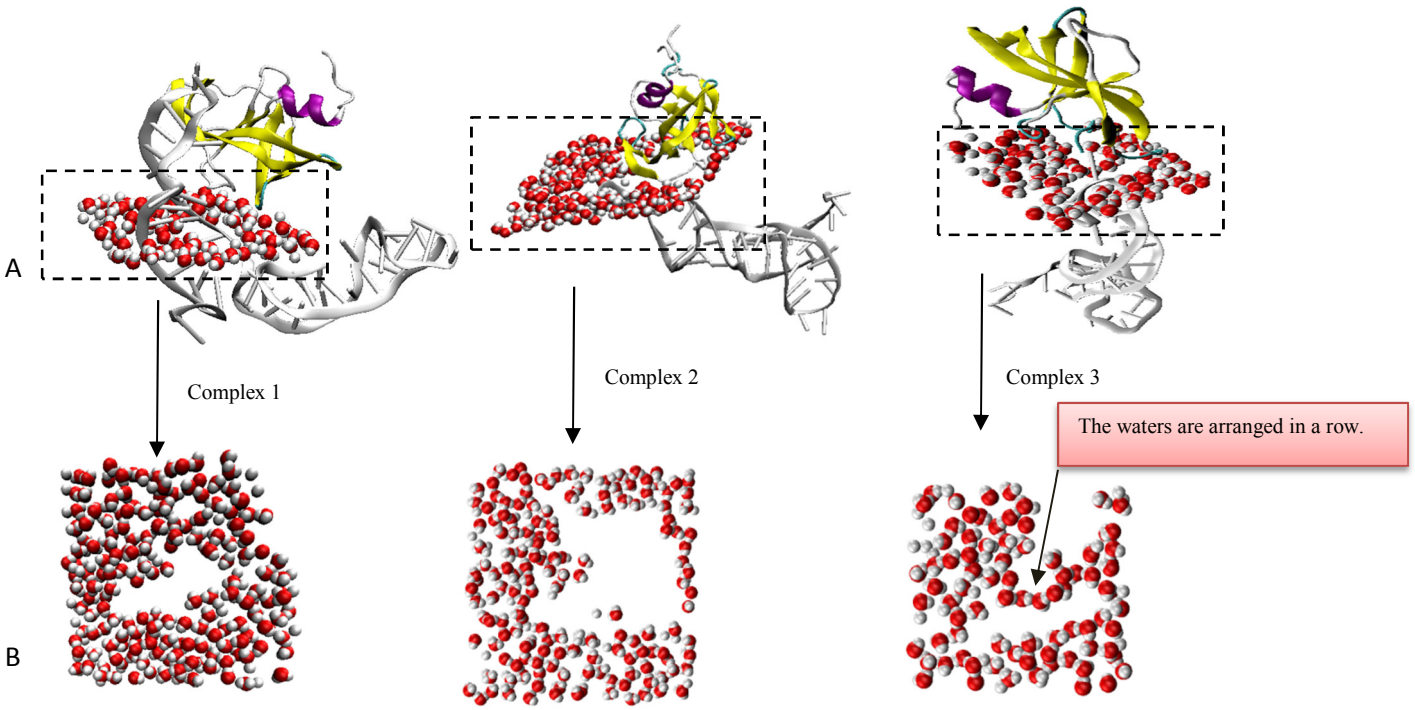

Figure12. Distribution of the water molecules between aptamer and protease for complex1, 2 and 3 in two states A and B.